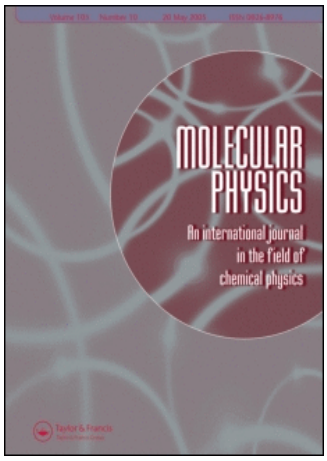

Molecular Physics
An International Journal in the Field of Chemical Physics
Publication details, including instructions for authors and subscription information:
http://www.informaworld.com/smpp/title~content=t713395160

Theoretical investigation of vibrational relaxation of NO($^2\Pi$), O), and N) in collisions with O(^{3}P)

M. V. Ivanov [a]
[a] Max-Planck-Institut für Dynamik und Selbstorganisation. D-37073 Göttingen. Germany

To cite this Article: Ivanov, M. V., Schinke, R. and Mcbane, G. C. , 'Theoretical investigation of vibrational relaxation of NO($^2\Pi$), O), and N) in collisions with O(^{3}P)', Molecular Physics, 105:9, 1183 - 1191
To link to this article: DOI: 10.1080/00268970701288087
URL: http://dx.doi.org/10.1080/00268970701288087

Molecular Physics, Vol. 105, No. 9, 10 May 2007, 1183–1191

Taylor & Francis
Taylor & Francis Group

Theoretical investigation of vibrational relaxation of $NO(^2\Pi)$, $O_2(^3\Sigma_g^-)$, and $N_2(^1\Sigma_g^+)$ in collisions with $O(^3P)$

M. V. IVANOV†, R. SCHINKE*† and G. C. MCBANE‡

†Max-Planck-Institut für Dynamik und Selbstorganisation, D-37073 Göttingen, Germany
‡Department of Chemistry, Grand Valley State University, Allendale, MI 49401, USA

(*Received 21 December 2006; in final form 16 February 2007*)

The vibrational relaxation of $NO(^2\Pi)$, $O_2(^3\Sigma_g^-)$, and $(^1\Sigma_g^+)$ in collisions with $O(^3P)$ is investigated by means of classical trajectories (NO, O_2) and quantum mechanical (N_2) scattering calculations N_2 using calculated potential energy surfaces. For NO and O_2, intermediate collision complexes are formed and the relaxation rate coefficients are large, of the order of $5 \times 10^{-11}\,cm^3\,s^{-1}$ and $2 \times 10^{-12}\,cm^3\,s^{-1}$, respectively, at room temperature. The agreement with available experimental data for NO is very good. The calculated rate coefficient for O_2, however, is about two times smaller than the measured rate coefficient. In both cases, the relaxation rate coefficient is slightly smaller than the complex formation or twice the atom exchange rate. Oxygen atoms colliding with N_2, on the other hand, do not form a collision complex; the potential energy surfaces for $N_2(^1\Sigma_g^+) + O(^3P)$ are purely repulsive. The calculated room temperature rate coefficient is on the order of $1 \times 10^{-15}\,cm^3\,s^{-1}$; it underestimates the measured rate coefficient by about a factor of 4.

Keywords: Vibrational relaxation; Diatom–atom collisions

1. Introduction

Vibrational relaxation of diatomic molecules in collisions with atoms or other molecules,

$$BC(v) + A \rightarrow BC(v' < v) + A, \qquad (1)$$

is an important process in several fields of physical chemistry, especially the chemistry of planetary atmospheres [1, 2]. The cross section or rate coefficient for vibrational relaxation is governed by the dependence of the interaction potential $V_I(R, r, \gamma) \equiv V(R, r, \gamma) - v_{BC}(r)$ on the vibrational coordinate r [3–5]. Here, R, r, and γ are the common Jacobi coordinates for a BC + A collision, V is the full potential energy surface (PES), and $v_{BC}(r)$ is the vibrational potential of the free BC molecule. For purely repulsive PESs the dependence of V_I on r is generally very weak with the consequence that vibrational relaxation is very slow. If, however, a long-lived intermediate collision complex is formed through strong attractive forces, the relaxation can be very fast [6, 7]. In such a case the BC bond may change drastically along the reaction path so that $\partial V_I/\partial r$ is large; the BC bond strength in the complex can be quite different from the bond strength of the free BC reactant. The transition along the reaction path from the region where translation and vibration are almost decoupled to the regime where both degrees of freedom are strongly coupled usually occurs in the vicinity of the transition state (TS).

If the lifetime of the collision complex is sufficiently long so that the internal energy is randomized, it is unlikely that vibrational energy will concentrate in the vibrational mode of the product diatom, i.e. the reactant molecule is effectively vibrationally deactivated [8]. In view of this picture it appears plausible to assume that the rate coefficient for vibrational relaxation, k^{vr}, is similar in magnitude to the rate coefficient for the formation of the collision complex, k^{cf}, which, in turn, is similar to the high-pressure recombination rate coefficient, k^r_∞ [7, 9, 10]. The latter is difficult to measure and therefore the measurement of k^{vr} is of great practical importance. The close relationship between k^{vr} and k^r_∞ has been illustrated for several collision systems (see [7] for examples).

Recently, we started to investigate the dynamics of $NO(^2\Pi) + O(^3P)$ collisions, with emphasis on the

*Corresponding author. Email: rschink@gwdg.de

Molecular Physics
ISSN 0026–8976 print/ISSN 1362–3028 online © 2007 Taylor & Francis
http://www.tandf.co.uk/journals
DOI: 10.1080/00268970701288087

O atom exchange reaction and NO_2 recombination [11]. Classical trajectories were calculated on two *ab initio* PESs, for the attractive $^2A'$ and the attractive $^2A''$ state, respectively. The agreement with experimental data for the exchange rate coefficient k^{ex} and the high-pressure recombination rate coefficient was good. In addition, the pressure and temperature dependence of the recombination rate k^r, calculated in a strong-collision model with the stabilization frequency as parameter, was also in good agreement with the experimental data. In the present paper we extend this study and calculate the rate coefficient for vibrational relaxation, i.e.

$$NO(^2\Pi, v) + O(^3P) \rightarrow NO(^2\Pi, v' < v) + O(^3P), \qquad (2)$$

with $v = 1, \ldots, 7$.

In a second application we calculate k^{vr} for

$$O_2(^3\Sigma_g^-, v = 1) + O(^3P) \rightarrow O_2(^3\Sigma_g^-, v = 0) + O(^3P). \qquad (3)$$

The kinetics of ozone has received much interest in recent years because of the unusual isotope effect [12]. Despite many detailed theoretical studies performed in the past decade, essential aspects of the complex formation, the O atom exchange, and the recombination are not well understood [13]. For example, classical trajectory calculations for the exchange reaction employing an accurate ground state PES [14] severely underestimated the rate coefficient [15]. Calculations for the vibrational relaxation of O_2 in collisions with O and comparison with recent experimental data will strengthen our understanding of this important molecular system.

In both collisions, $NO + O$ and $O_2 + O$, long-lived complexes are formed and therefore the relaxation rates are large. Classical mechanics is an appropriate tool for investigating these two systems. In order to contrast them with a system which does not proceed via a complex, we perform additional calculations for a system with a purely repulsive PES, namely

$$N_2(^1\Sigma_g^+, v = 1) + O(^3P) \rightarrow N_2\left(^1\Sigma_g^+, v = 0\right) + O(^3P). \qquad (4)$$

The corresponding rate coefficient is several orders of magnitude smaller than for reactions (2) and (3). The relaxation of N_2 in collisions with O atoms is a classically forbidden process, in the sense of classical *S*-matrix theory [16], and requires a quantum mechanical description; classical trajectories yield a vanishing rate coefficient at room temperature.

2. Calculations

2.1. *Potential energy surfaces*

For NO_2, only the states $1\,^2A'$ and $1\,^2A''$ are attractive and have to be taken into account in (2). The PESs have been determined by Kurkal *et al.* [17] and Ivanov *et al.* [11] and are used in the present application without modification. The first excited $2\,^2A'$ state also has a deep potential well and correlates with $NO(^2\Pi) + O(^3P)$. However, a relatively high reaction barrier ($\sim$0.19 eV [17]) hinders the formation of a NO_2 complex and therefore the $2\,^2A'$ state is not expected to significantly contribute to the relaxation process, especially not at room temperature. It is not included in the present investigation. The same holds true for the many other repulsive states correlating with $NO(^2\Pi) + O(^3P)$ [11].

Figures 1(a) and (b) show two-dimensional contour plots of the $^2A'$ and $^2A''$ PESs of NO_2 for fixed ONO bond angle α; R_1 and R_2 are the two NO bond distances. Both PESs are strongly attractive and, of course, symmetric with respect to the interchange of the two O atoms. The weakening of the NO vibrational bond inside the potential well is quite obvious.

The PES of the ground state of ozone, $^1A'$, has been calculated by Siebert *et al.* [14, 18]. It has a very small reaction barrier, which clearly determines the TS between the ozone well and the reactant region. This barrier depends on the level of electronic structure theory, especially the atomic basis set [15, 19]. In the present study we use the modification of the original PES due to Babikov *et al.* [20]. Figure 1(c) shows a two-dimensional representation of the ozone PES for fixed OOO bond angle; here, R_1 and R_2 are the two bond distances between the central O atom and the two end atoms. The O_3 PES is much less attractive than the NO_2 PESs. Actually, it has a 'reef' structure around $R_1 \sim 3.8a_0$, i.e. a small barrier below the dissociation threshold. As a consequence of this 'reef' the TS is much narrower than for the two NO_2 PESs.

Three different triplet states, $1\,^3A'$ and $1, 2\,^3A''$, emerge from the reactants $N_2(^1\Sigma_g^+) + O(^3P)$. The corresponding PESs [21] are purely repulsive and do not lead to the formation of N_2O complexes like the PESs for NO_2 and O_3. The linear ground state of $N_2O(\tilde{X}\,^1A')$ asymptotically correlates with excited oxygen atoms, i.e. $N_2(X\,^1\Sigma_g^+) + O(^1D)$, rather than the ground state products $N_2(^1\Sigma_g^+) + O(^3P)$. A collision complex can be formed only via spin–orbit (SO) coupling between the triplet states and the singlet ground state, which cross at intermediate N_2–O separations [21, 22]. SO interaction is not taken into account in the present study and therefore the possibility of forming N_2O complexes is neglected.

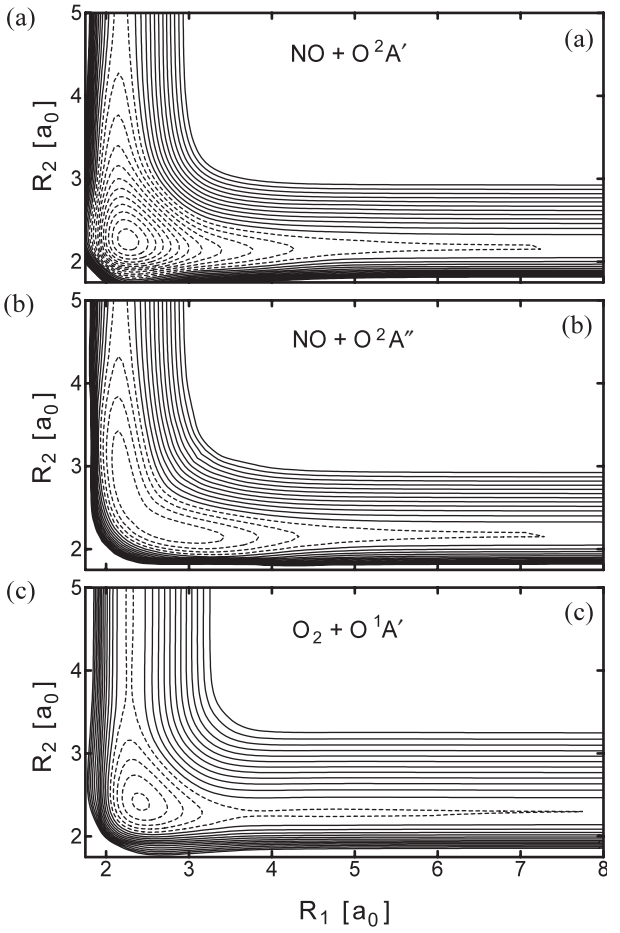

Figure 1. (a) Contour plot of the ^{2}A′ PES of NO_2 as a function of the two NO bond distances R_1 and R_2 for bond angle $\alpha = 134.5°$. (b) Contour plot of the ^{2}A″ PES of NO_2 as a function of the two NO bond distances for $\alpha = 110.1°$. (c) Contour plot of the ^{1}A′ PES of O_3 as function of the two OO bond distances R_1 and R_2 for bond angle $\alpha = 116.8°$. In all figures the spacing between the contours is 0.25 eV and the highest contour is for $E = 3$ eV. Energy normalization is such that $E = 0$ corresponds to BC + O with BC (NO and O_2) at equilibrium. Contours for positive energies are indicated by solid lines and contours for negative energies (including $E = 0$) are shown by the dashed lines.

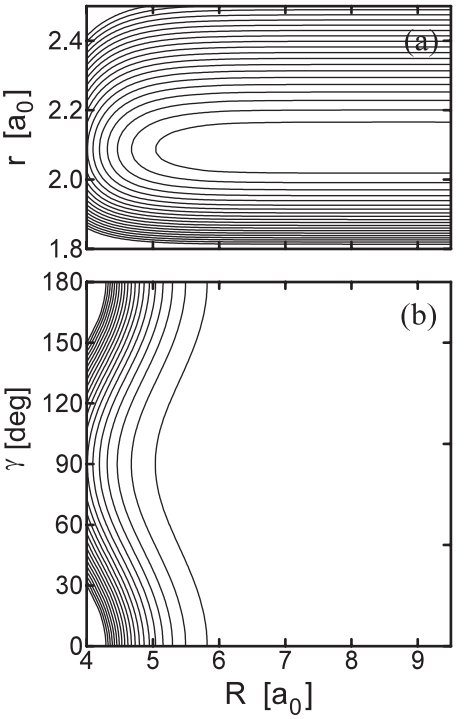

Figure 2. Contour plots of the ^{3}A′ PES of N_2O as a function of the Jacobi coordinates R and r (a) and R and γ (b). In (a) $\gamma = 90°$ and in (b) $r = 2.09a_0$. The spacing between the contours is 0.1 eV and the highest contour is for $E = 2$ eV. Energy normalization is such that $E = 0$ corresponds to N_2 + O with N_2 at equilibrium.

In the present calculations, vibrational relaxation of $N_2(v = 1)$ can be induced only by the r dependence of the repulsive triplet potentials.

PESs for the lowest three triplet states have been determined previously by Nakamura and Kato [21]. In the present work, we use PESs calculated by the full-valence complete active space self-consistent field (CASSCF) method [23, 24]. The active space included the 2s and 2p orbitals (16 electrons in 12 orbitals), whereas the 1s orbitals were kept doubly occupied but optimized in the CASSCF procedure. The lowest ^{3}A′ and the two lowest ^{3}A″ states were calculated simultaneously. Dunning's standard augmented correlation consistent polarization triple zeta (aug-cc-pVTZ) atomic basis set was used [25]. All electronic structure calculations were performed with the MOLPRO suite of programs [26]. The purpose of the calculations for reaction (4) is to demonstrate the smallness of the relaxation rate coefficient in cases where no 'chemically' bound collision complex is formed; the CASSCF PESs are sufficiently accurate for this purpose.

For the construction of the PESs the Jacobi coordinates appropriate for N_2 + O were varied: R ranges from $3.5a_0$ to $10a_0$ with $\Delta R = 0.25a_0$; for r the values (in a_0) 1.8, 1.9, 2.0, 2.1, 2.2, 2.4, 2.6, and 2.8 are chosen; and the angle γ is varied from 0 to 90° with $\Delta\gamma = 10°$. Interpolation between the grid points is done by three-dimensional cubic splines. Two-dimensional plots of the PES of state ^{3}A′ are depicted in figure 2. Plots for the other two PESs are very similar. The potentials are repulsive and the translational (R)/vibrational (r) coupling is exceedingly weak.

2.2. *Trajectory calculations for NO + O and O_2 + O collisions*

The classical trajectory calculations for NO + O and O_2 + O collisions were performed in the same way as

described, for example, in [11]. The only difference is that, initially, the reactant molecule has the appropriate vibrational energy corresponding to a specific quantum state v of BC. The other initial coordinates and momenta are selected randomly from appropriate thermal distributions. The vibrational relaxation rate coefficient for a transition $v \rightarrow v'$ is then calculated according to

$$k^{\mathrm{vr}}(v \rightarrow v') = g(T)^{-1}\pi b_{\max}^2 \left(\frac{8k_{\mathrm{B}}T}{\pi\mu}\right)^{1/2} \frac{N_{\mathrm{vr}}(v \rightarrow v')}{N_{\mathrm{tot}}}, \quad (5)$$

where N_{tot} is the total number of trajectories and $N_{\mathrm{vr}}(v \rightarrow v')$ is the number of trajectories that made a transition from state v to v'. In the present calculations we employed a simple boxing procedure. After the trajectory is terminated the vibrational energy E'_{vib} is determined. If $(\epsilon_{v'-1} + \epsilon_{v'})/2 \leq E'_{\mathrm{vib}} \leq (\epsilon_{v'+1} + \epsilon_{v'})/2$, where $\epsilon_{v'}$ is the quantum mechanical energy of state v', BC is considered to be in state v'. $g(T)$ is the electronic degeneracy factor, which accounts for the many SO states which are repulsive and therefore do not contribute much to k^{vr}. The appropriate expressions for reactions (2) and (3) are given, for example, by Harding *et al.* [27] and Gross and Billing [28], respectively. The maximum impact parameter was $b_{\max} = 8$ Å in all calculations for NO + O and O_2 + O and typically 7000 trajectories were calculated for each temperature. For NO + O the calculations were performed for both electronic states separately and the rate coefficients were then added.

2.3. *Quantum mechanical calculations for N_2+O collisions*

Three different triplet states emerge from $N_2(^1\Sigma_g^+) + O(^3P)$. We performed quantum mechanical (as well as classical trajectory) scattering calculations only for the $^3A'$ PES and assumed that the rate coefficients for the other states have the same magnitude. In other words, we considered the electronic degeneracy factor to be $g(T) = 1$.

The scattering calculations were carried out with a parallel version [29] of the MOLSCAT program [30], and the coupled states approximation [31] was employed. They require radial strength functions $V_{vjv'j'\lambda}(R)$ such that

$$\langle\phi_{vj}(r)|V_I(R,r,\gamma)|\phi_{v'j'}(r)\rangle = \sum_{\lambda} V_{vjv'j'\lambda}(R)P_\lambda(\cos\gamma), \quad (6)$$

where the $\phi_{vj}(r)$ are vibrational wavefunctions of N_2 in the internal state labeled by v and j, P_λ is a Legendre polynomial, and the brackets indicate integration over the diatomic bond length coordinate r. We obtained the interaction potential from the splined 3D potential described above by substituting $V(100a_0, r, \gamma)$ for $v_{\mathrm{BC}}(r)$. We then obtained the radial strength functions by quadrature according to

$$V_{vjv'j'\lambda}(R) = \left(\lambda + \frac{1}{2}\right)^{1/2} \int_{-1}^{1} \mathrm{d}x\, P_\lambda(x) \langle\phi_{vj}(r)|V_I(R,r,x)|\phi_{v'j'}(r)\rangle, \quad (7)$$

where $x = \cos\gamma$. For the integral over r we used a seven-point Gauss–Hermite quadrature. Our angular expansion included even values of λ through $\lambda = 20$; we used a 32-point Gauss–Legendre quadrature in $\cos\gamma$.

To determine the diatomic vibrational wavefunctions $\phi_{vj}(r)$ we used the recent N_2 potential curve of Le Roy *et al.* [32], evaluated with code from Le Roy's LEVEL program [33], and the discrete variable representation method of Balint-Kurti *et al.* [34]. Separate vibrational functions $\phi_{vj}(r)$ were computed for each rovibrational state; that is, centrifugal distortion was included in the diatomic wavefunctions. Asymptotic channel energies for the N_2 levels were determined with the same N_2 potential and the LEVEL program.

The rovibrational basis set for the scattering calculations included all N_2 levels with energies below 6000 cm^{-1} for calculations at total energies of 5500 cm^{-1} and below. For total energies between 5600 and 8000 cm^{-1}, all levels with energies below 8500 cm^{-1} were included in the basis. These criteria yielded basis sets that included vibrational states $v = 0$, 1, and 2 at 5500 cm^{-1} and below, and $v = 0$–3 above 5500 cm^{-1}. In all cases, at least one closed rotational level for each v was present in the basis. Only even Δj transitions are possible for N_2, so separate calculations were performed with basis sets containing only even or odd j levels.

The coupled channel equations were propagated with the hybrid log-derivative/Airy propagator of Alexander and Manolopolous [35]. The partial wave sum included all orbital angular momenta up to $l = 180$ at the lower total energies and up to $l = 220$ above 5500 cm^{-1}. These maximum values of l are adequate to converge all the vibrationally inelastic cross sections to better than 1%. In the calculations above 5500 cm^{-1}, the coupled equations were solved for only every other l, and the cross sections multiplied by two to compensate.

State-to-state rate coefficients were computed by thermal averages over collision energy,

$$k(v, j \rightarrow v', j') = \left(\frac{8k_{\mathrm{B}}T}{\pi\mu}\right)^{1/2} \left(\frac{1}{k_{\mathrm{B}}T}\right)^2 \int_0^\infty E_{\mathrm{c}}\sigma_{v,j\rightarrow v',j'}(E_{\mathrm{c}}) \exp(-E_{\mathrm{c}}/k_{\mathrm{B}}T)\mathrm{d}E_{\mathrm{c}}, \quad (8)$$

where the collision energy $E_c = E_{tot} - \epsilon_{vj}$. The cross sections were computed on an energy grid with 50 cm^{-1} spacing below 4050 cm^{-1}, 100 cm^{-1} spacing between 4100 and 5600 cm^{-1}, and 200 cm^{-1} spacing up to the maximum total energy of 8000 cm^{-1}. (The energy of the $v=1, j=0$ level is 2329.912 cm^{-1}.) The integral over collision energy was performed on this grid by the overlapping parabolas method [36]. We then averaged the state-to-state rate coefficients over the initial states and summed over all final states to obtain $k^{vr}(T)$.

3. Results

3.1. *NO+O*

Before we discuss the relaxation rate coefficients we first show in figure 3 for the $^2A'$ PES the impact parameter-dependent probabilities defined as $P(1 \rightarrow 0 \mid b) = N_{vr}(1 \rightarrow 0 \mid b)/N_{tot}(b)$. They are more or less constant for smaller values of b, increase slightly to a maximum and then very quickly decay to zero. The corresponding probabilities for complex formation exhibit similar behaviour as a function of the impact parameter. They are, of course, larger than the $P(1 \rightarrow 0 \mid b)$, because not every trajectory automatically leads to vibrational relaxation. No complexes are formed beyond the maximum with the result that the probability for vibrational relaxation also goes to zero. The maximum probability as well as the maximum impact parameter for which relaxation still occurs decreases with collision energy E_c with the consequence that the cross sections (not shown) also decrease with E_c. The probabilities for the $^2A''$ PES are similar.

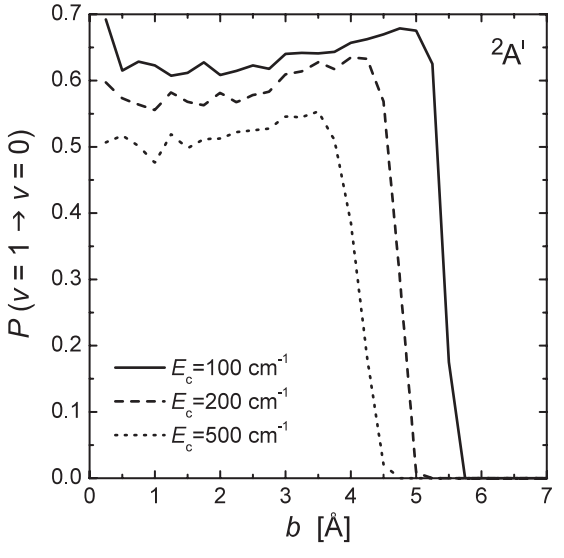

Figure 3. Impact parameter-dependent probabilities $P(1 \rightarrow 0 \mid b)$ (see the text for definition) for vibrational relaxation calculated for the $^2A'$ PES of NO_2.

Figure 4 shows the calculated relaxation rate coefficients for NO + O as a function of temperature in comparison with the available experimental data. Because of the strong attraction the complex formation rate coefficient (calculated in [11]) is large and so is k^{vr}. The temperature dependence of k^{vr} is approximately described by $T^{-0.4}$ over the entire temperature range. Because the intramolecular energy randomization in highly excited NO_2 complexes is fast [37, 38], it is expected that k^{vr} will be similar to k^{cf}, which, in turn, is $\sim 2k^{ex}$, and figure 4 confirms this. Nevertheless, k^{vr} is slightly but systematically smaller than $k^{cf} \approx 2k^{ex}$ for all temperatures.

The most recent experimental results are those of Hwang *et al.* [39]. The agreement with the calculated rates is very good over the entire range of temperatures for which measurements have been performed. The early result of Fernando and Smith [40] for room temperature is slightly higher than the calculated value. The calculated k^{vr} is also in reasonable agreement with the high-temperature result of Glänzer and Troe [41] obtained in shock waves. Small contributions from state $2\,^2A'$, whose PES has a reaction barrier of about

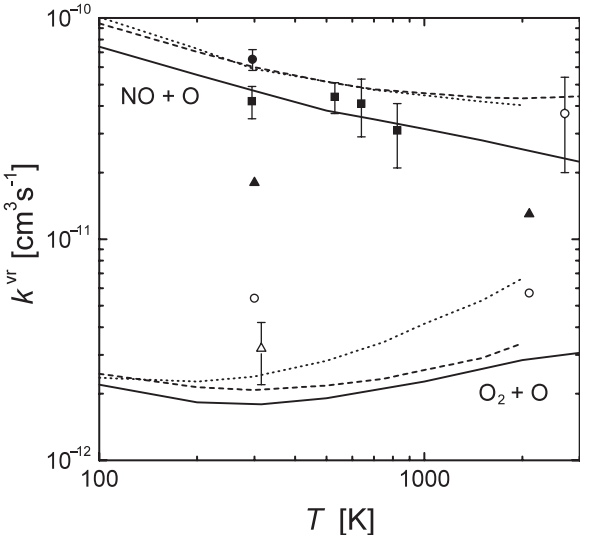

Figure 4. Calculated vibrational relaxation rate coefficients (solid lines) for NO + O and O_2 + O vs. temperature. Also shown are the rate coefficients k^{cf} for complex formation (dotted lines) and two times the rate coefficients k^{ex} for the exchange reactions (dashed lines). The black triangles (▲) and open circles (○) indicate the results of Quack and Troe [43] for NO + O and O_2 + O, respectively. The experimental data (symbols with error bars) are taken from: Hwang *et al.* [39] (■), Fernando and Smith [40] (●), Glänzer and Troe [41] (○), and Kalogerakis *et al.* [45] (△).

0.19 eV (~2200 K), cannot be excluded in this temperature range.

Duff and Sharma [42] performed classical trajectory calculations using analytical model PESs for the $^2A'$ and $^2A''$ states. Their values of $k^{vr} \approx 3 \times 10^{-11}$ cm^3 s^{-1}, more or less independent of temperature from 300 K to about 3000 K, are slightly smaller than our and the experimental data, especially at low T. Quack and Troe [43] used a statistical approach to determine k^{vr}. Their predictions for 300 K and 2100 K, also included in figure 4, are significantly smaller than the experimental rate coefficients. Nevertheless, in view of the simplicity of the statistical approach, the agreement within a factor of 4 is noteworthy.

Hwang *et al.* [39] also determined (for room temperature) the removal rate coefficient of NO($v = 2$), i.e.

$$k^{vr}(v) = \sum_{v'<v} k^{vr}(v \rightarrow v'), \tag{9}$$

with $v = 2$. The calculated results for v up to 7 are shown in figure 5 together with the experimental results. Except for the result for $v = 2$ the calculated removal rates gradually increase with v. The two experimental points also suggest an increase with v, although the error bars are large. An increase with v was also obtained by Duff and Sharma [42]. The analysis of the trajectories shows that the increase with v is not due to an increase of the complex formation rate coefficient. This indicates that the increased relaxation rate is the result of more efficient energy transfer in the complex.

For completeness, we show in figure 6 the full 'matrix' of rate coefficients $k^{vr}(v \rightarrow v')$ for room temperature. For a given initial state v the state resolved rate coefficients depend only slightly on the final vibrational state v'. Duff and Sharma [42] obtained qualitatively similar results. Analysis of the trajectories indicates that the average complex survival time increases slightly with decreasing Δv, i.e. the larger v' the longer the lifetime. This might explain the observation that, generally, the relaxation rate coefficient increases with v' for a particular initial state v.

3.2. $O_2 + O$

The vibrational relaxation rate coefficient for reaction (3) is also shown in figure 4. It is almost temperature independent up to about 600 K and then rises slightly to the high-temperature region by roughly a factor of 2. Also shown are the complex formation rate coefficient k^{cf} and $2k^{ex}$. While for NO + O $k^{cf} \approx 2k^{ex}$ for the entire temperature range, this holds true for $O_2 + O$ only for lower values of T. At higher temperatures (collision energies) $O_2 + O$ collisions gradually become less statistical and direct back scattering into the reactant channel becomes more pronounced [44]. The relaxation rate coefficient is only slightly smaller than $2k^{ex}$ over the entire temperature range. For $O_2 + O$ only one state out of 27 states is attractive and leads to complex formation, while for NO + O a total of four states (two two-fold

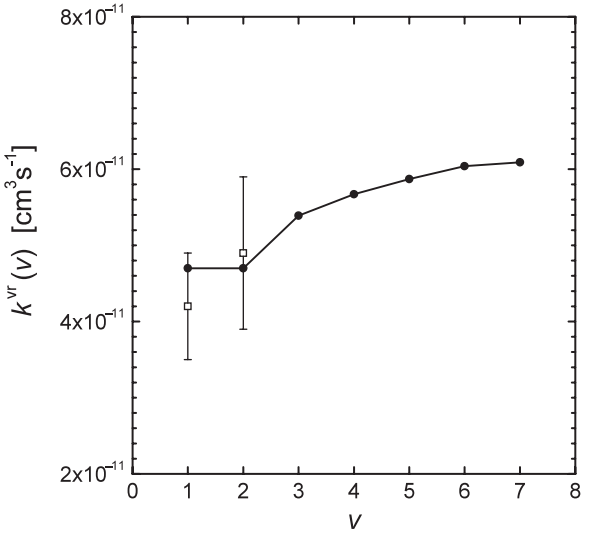

Figure 5. Calculated removal rates $k^{vr}(v)$ for NO + O and $T = 300$ K as a function of the initial vibrational state v. The open squares are the measured room temperature results of Hwang *et al.* [39].

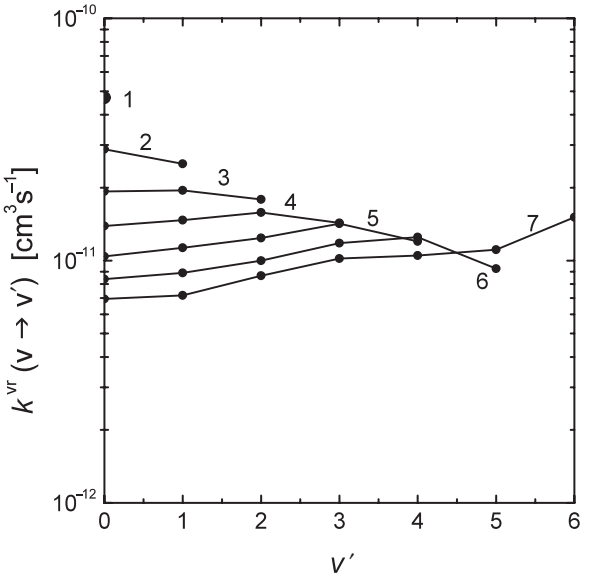

Figure 6. Final state resolved relaxation rate coefficients $k^{vr}(v \rightarrow v')$ for NO + O and room temperature.

degenerate states) out of 36 states lead to complex formation. That is, the statistical factor $g(T)^{-1}$ in equation (5) for O_3 is about three times smaller than for NO_2. This partly explains the large difference between the relaxation rates for $O_2 + O$ and $NO + O$ in figure 4. The main difference between $O_2 + O$ and $NO + O$ is, however, the different topographies of the PESs: while the two PESs for $NO + O$ are purely attractive with a wide TS, the PES for $O_2 + O$ has a reef structure with a narrow TS.

The most recently measured rate coefficient at room temperature [45] is clearly larger than the calculated k^{vr}. The ratio of about two is, however, smaller than the corresponding ratio for the exchange rate coefficient, which around 300 K is of the order of 2.5–3 [15]. Nevertheless, compared with $NO + O$ the agreement with the experimental relaxation rate coefficient is rather poor, which indicates that something is missing in the one-state classical model. It is important to note that, except for the ground state, all states that correlate with $O_2(^3\Sigma_g^-) + O(^3P)$ are highly repulsive and do not lead to O_3 complexes [46]. Therefore, contributions to the vibrational relaxation rate coefficient are expected to be marginally small.

A possible explanation for the underestimation is the neglect of non-adiabatic coupling between the many states in the reactant channel [11]. Including this coupling may increase k^{cf} and thus the vibrational relaxation as well as the exchange rate coefficient. In [11] we discussed this question on the basis of the potential energy surfaces in the entrance channel for $NO + O$ and $O_2 + O$ [46].

The only other calculated rate coefficient for $O + O_2$ we are aware of is the one of Quack and Troe [43] obtained by a simple statistical model (figure 4). The value for 300 K is significantly larger than the rate coefficient calculated in the present work and it is also larger than the experimental value.

3.3. $N_2 + O$

Vibrational relaxation for $N_2 + O$ is so slow that, at room temperature, no classical trajectory out of several millions of trajectories (with $b_{max} = 5$ Å) has been found that could be classified as relaxation, i.e. the classical relaxation rate coefficient is practically zero. The experimental rate coefficient for 300 K is 3.2×10^{-15} cm^3 s^{-1} [47]. For much higher temperatures the classical calculations do yield a non-zero relaxation rate. For example, the calculated rate at 3000 K is of the order of 2×10^{-14} cm^3 s^{-1}. However, this is still more than one order of magnitude smaller than the corresponding experimental rate coefficient of 4×10^{-13} cm^3 s^{-1} [48].

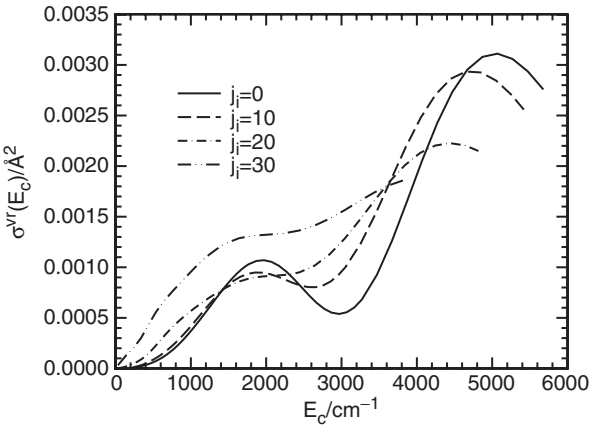

Figure 7. Quantum mechanical $1 \rightarrow 0$ relaxation cross sections for selected initial rotational states j_i as a function of the collision energy E_c.

The quantum mechanical relaxation cross sections, although small, are non-zero even at low collision energies. In figure 7 we show for selected initial rotational states j vibrational relaxation cross sections summed over the final rotational states of $N_2(v = 0)$, $\sigma_j^{vr}(E_c)$. All cross sections rapidly rise with increasing E_c; in the high-energy range some cross sections develop undulations. In the low-energy onset the cross sections gradually increase with initial rotation. The calculated room temperature rate coefficient using the CS cross sections is 0.8×10^{-15} cm^3 s^{-1}, about four times smaller than the measured rate coefficient [47]. In view of the smallness of the cross sections this level of agreement is reasonable; small changes of the PES, for example, are likely to have a large effect on the rate coefficient. The calculated k^{vr} rapidly increases with temperature; it is, for example, 5.8×10^{-15} cm^3 s^{-1} at 723 K. However, the experimental rate coefficient increases even faster with T; it is 4.0×10^{-14} cm^3 s^{-1} at the same temperature [47].

4. Discussion and summary

The present calculations for $NO(v = 1) + O$ and $O_2(v = 1) + O$ provide further evidence for the general view that vibrational relaxation is fast if an intermediate collision complex is formed. Under such circumstances, vibrational relaxation is governed by the association of the atom and the diatom and the relaxation rate coefficient k^{vr} is of similar magnitude as the complex formation rate coefficient k^{cf}. The agreement of the classical trajectory calculations for $NO + O$ using accurate PESs for the two attractive electronic states is good. On the other hand, similar calculations for

$O_2 + O$ yield a relaxation rate coefficient which is about a factor of 2 smaller than the measured value. This discrepancy can have two major causes: the failure of classical mechanics, especially the crude binning procedure of the trajectories into two vibrational 'boxes', or the neglect of non-adiabatic coupling to other (repulsive) states in the entrance channel, which could enhance complex formation and therefore k^{vr}. If the classical description were responsible for the underestimation of k^{vr}, it would equally affect the calculations for $NO + O$, which seems not to be the case, however. Therefore, we interpret the present results as additional support for the hypothesis that the correct description of collisions between O atoms and O_2 diatoms requires a more accurate treatment of the coupling between the states correlating with $O_2(^3\Sigma_g^-) + O(^3P)$ [11, 13].

If the intermediate collision complexes are long-lived so that the energy is more or less equilibrated among the internal degrees of freedom, k^{vr} should be slightly smaller than two times the exchange rate coefficient. The calculated rates reasonably fulfill this relationship, but the measured ones do not. For $NO + O$ and 300 K, $2k^{ex}$ is $7.4 \times 10^{-11}\,cm^3\,s^{-1}$ [49], whereas $k^{vr} = 4.2 \times 10^{-11}\,cm^3\,s^{-1}$ [39]. Likewise, two times the exchange rate coefficient for $O_2 + O$ and 300 K is $6 \times 10^{-12}\,cm^3\,s^{-1}$ [44] and $k^{vr} = 3.2 \times 10^{-12}\,cm^3\,s^{-1}$ [45]. Even though the experimental uncertainties are large for all four rate coefficients, there seems to be a systematic trend that k^{vr} is clearly smaller than $2k^{ex}$.

The third example of the present investigation, $N_2 + O$, exemplifies very slow vibrational relaxation in cases when the PES is purely repulsive and no intermediate complex is formed. The rate coefficient is several orders of magnitude smaller than for complex forming collisions and shows a strong positive temperature dependence. Because of the smallness of the cross sections, ordinary classical trajectory calculations are not adequate and quantum mechanical calculations are required. The calculated room temperature k^{vr} is smaller by a factor of 4 than the experimental value and this factor increases with T. The underestimation can be due to a failure of the PES, which is not implausible in view of the low level of electronic structure theory, or by the neglect of complex formation in the N_2O ground state $\tilde{X}\,^1\Sigma^+$ due to spin–orbit coupling between the triplet states and the singlet state. The latter was roughly modeled by Fisher and Bauer [50]. However, the lowest singlet–triplet crossing point is at least 1 eV above the $N_2 + O$ asymptote and, moreover, the SO coupling element is only of the order of $80\,cm^{-1}$ [21]. Therefore, this 'chemical' mechanism for vibrational relaxation of N_2 in collisions with O atoms [50] appears not to be important for temperatures below 1000 K or so. Another possible relaxation mechanism is vibronic interaction among the triplet states at crossings of vibrationally adiabatic potentials belonging to different electronic states [51, 52]. An assessment of this mechanism goes far beyond the level of the present calculations. Before extensive multi-state scattering calculations are tackled, however, one should first calculate accurate triplet state PESs.

The vibrational relaxation of $CO(^1\Sigma^+)$ in collisions with $O(^3P)$ is an interesting example intermediate between the adiabatic and the chemical mechanisms. Two of the triplet states that correlate with $CO(^1\Sigma^+) + O(^3P)$ have sizable potential wells but also reaction barriers of 0.2 eV and 0.3 eV, respectively [53]. As in N_2O, the $^1A'$ ground state does not correlate with the ground state products. The measured rate coefficient at room temperature is of the order of $k^{vr} = 3 \times 10^{-14}\,cm^3\,s^{-1}$ [54] and increases by about two orders of magnitude for temperatures around 1000 K [55]. Classical trajectory calculations underestimate k^{vr} by an order of magnitude at low temperatures but agree well with the large rate coefficients at high temperatures, which are determined by complex forming collisions [53].

Acknowledgements

Financial support from the Deutsche Forschungsgemeinschaft is gratefully acknowledged. GCM is grateful to R. J. Le Roy for a code evaluating the N_2 potential. This research was supported, in part, by the U.S. National Science Foundation through the San Diego Supercomputer Center.

References

[1] T. L. Cottrell and J. C. McCoubrey, *Molecular Energy Transfer in Gases* (Butterworth, London, 1961).
[2] E. Weitz and G. Flynn, A. Rev. Phys. Chem. **25,** 275 (1974).
[3] D. Rapp and T. Kassal, Chem. Rev. **69,** 61 (1969).
[4] F. A. Gianturco, *The Transfer of Molecular Energy by Collisions* (Springer, Heidelberg, 1979).
[5] A. S. Dickinson, Comput. Phys. Commun. **17,** 51 (1979).
[6] R. P. Fernando and I. W. M. Smith, J. Chem. Soc. Faraday Trans. 2 **77,** 459 (1981).
[7] I. W. M. Smith, J. Chem. Soc. Faraday Trans. **93,** 3741 (1997).
[8] Y. Liu, L. L. Lohr, and J. R. Barker, J. Phys. Chem. A **110,** 1267 (2006).
[9] M. Quack and J. Troe, Ber. Bunsenges. Phys. Chem. **79,** 170 (1975).
[10] J. Troe, Chem. Rev. **103,** 4565 (2003).
[11] M. V. Ivanov, H. Zhu, and R. Schinke, J. Chem. Phys. **126,** 054304 (2007).
[12] K. Mauersberger, D. Krankowsky, C. Janssen, and R. Schinke, Adv. At. Molec. Opt. Phys. **50,** 1 (2005).

[13] R. Schinke, M. V. Ivanov, S. Yu. Grebenshchikov, and P. Fleurat-Lessard, Ann. Rev. Phys. Chem. **57,** 625 (2006).
[14] R. Siebert, P. Fleurat-Lessard, R. Schinke, M. Bittererová, and S. C. Farantos, J. Chem. Phys. **116,** 9749 (2002).
[15] P. Fleurat-Lessard, S. Yu. Grebenshchikov, R. Siebert, R. Schinke, and N. Halberstadt, J. Chem. Phys. **118,** 610 (2003).
[16] W. H. Miller, Chem. Phys. Lett. **7,** 431 (1970).
[17] V. Kurkal, P. Fleurat-Lessard, and R. Schinke, J. Chem. Phys. **119,** 1489 (2003).
[18] R. Siebert, R. Schinke, and M. Bittererová, Phys. Chem. chem. Phys. **3,** 1795 (2001).
[19] R. Schinke and P. Fleurat-Lessard, J. Chem. Phys. **121,** 5789 (2004).
[20] D. Babikov, B. K. Kendrick, R. B. Walker, R. T. Pack, P. Fleurat-Lessard, and R. Schinke, J. Chem. Phys. **118,** 6298 (2003).
[21] H. Nakamura and S. Kato, J. Chem. Phys. **110,** 9937 (1999).
[22] A. H. H. Chang and D. R. Yarkony, J. Chem. Phys. **99,** 6824 (1993).
[23] H.-J. Werner and P. J. Knowles, J. Chem. Phys. **82,** 5053 (1985).
[24] P. J. Knowles and H.-J. Werner, Chem. Phys. Lett. **115,** 259 (1985).
[25] T. H. Dunning, Jr, J. Chem. Phys. **90,** 1007 (1989).
[26] H.-J. Werner, P. J. Knowles, R. Lindh, M. Schütz, P. Celani, T. Korona, F. R. Manby, G. Rauhut, R. D. Amos, A. Bernhardsson, A. Berning, D. L. Cooper, M. J. O. Deegan, A. J. Dobbyn, F. Eckert, C. Hampel, G. Hetzer, A. W. Lloyd, S. J. McNicholas, W. Meyer, M. E. Mura, A. Nicklass, P. Palmieri, R. Pitzer, U. Schumann, H. Stoll, A. J. Stone, R. Tarroni, and T. Thorsteinsson. Molpro, version 2002.6, a package of *ab initio* programs, 2003. See http://www.molpro.net
[27] L. B. Harding, H. Stark, J. Troe, and V. G. Ushakov, Phys. Chem. Chem. Phys. **1,** 63 (1999).
[28] A. Gross and G. D. Billing, Chem. Phys. **217,** 1 (1997).
[29] G. C. McBane, Grand Valley State University, 2005. 'PMP Molscat', a parallel version of Molscat version 14 available at http://faculty.gvsu.edu/mcbaneg/pmpmolscat
[30] J. M. Hutson and S. Green, MOLSCAT computer code, version 14, 1994. Distributed by Collaborative Computational Project No. 6 of the Engineering and Physical Sciences Research Council (UK).
[31] P. McGuire and D. J. Kouri, J. Chem. Phys. **60,** 2488 (1974).
[32] R. J. Le Roy, Y. Huang, and C. Jary, J. Chem. Phys. **125,** 164310 (2006).
[33] R. J. Le Roy, Level 7.7: A computer program for solving the radial Schrödinger equation for bound and quasibound levels. Chemical Physics Research Report CP-661, University of Waterloo, 2005. See the 'Computer Programs' link at http://leroy.uwaterloo.ca
[34] G. G. Balint-Kurti, R. N. Dixon, and C. C. Marston, Int. Rev. Phys. Chem. **11,** 317 (1992).
[35] M. H. Alexander and D. E. Manolopoulos, J. Chem. Phys. **86,** 2044 (1987).
[36] R. E. Jones, Approximate integrator of functions tabulated at arbitrarily spaced abscissas. Technical Report SC-M-69-335, Sandia Laboratories, 1969. Implemented in the SLATEC program library as subroutine DAVINT.
[37] S. Yu. Grebenshchikov, H. Flöthmann, R. Schinke, I. Bezel, C. Wittig, and S. Kato, Chem. Phys. Lett. **285,** 410 (1998).
[38] M. V. Ivanov and R. Schinke, to be published.
[39] E. S. Hwang, K. J. Castle, and J. A. Dodd, J. Geophys. Res. **108,** 1109 (2003).
[40] R. P. Fernando and I. W. M. Smith, Chem. Phys. Lett. **66,** 218 (1979).
[41] K. Glänzer and J. Troe, J. Chem. Phys. **63,** 4352 (1975).
[42] J. W. Duff and R. D. Sharma, J. Chem. Soc. Faraday Trans. **93,** 2645 (1997).
[43] M. Quack and J. Troe, Ber. Bunsenges. Phys. Chem. **81,** 160 (1977).
[44] P. Fleurat-Lessard, S. Yu. Grebenshchikov, R. Schinke, C. Janssen, and D. Krankowsky, J. Chem. Phys. **119,** 4700 (2003).
[45] K. S. Kalogerakis, R. A. Copeland, and T. G. Slanger, J. Chem. Phys. **123,** 194303 (2005).
[46] M. Tashiro and R. Schinke, J. Chem. Phys. **119,** 10186 (2003).
[47] R. J. McNeal, M. E. Whitson, Jr, and G. R. Cook, J. Geophys. Res. **79,** 1527 (1974).
[48] D. J. Eckstrom, J. Chem. Phys. **59,** 2787 (1973).
[49] S. M. Anderson, F. S. Klein, and F. Kaufmann, J. Chem. Phys. **83,** 1648 (1985).
[50] E. R. Fisher and E. Bauer, J. Chem. Phys. **57,** 1966 (1972).
[51] E. E. Nikitin and S. Ya. Umanski, Faraday Discuss. Chem. Soc. **53,** 7 (1972).
[52] I. W. M. Smith, Accts Chem. Res. **9,** 161 (1976).
[53] M. Braunstein and J. W. Duff, J. Chem. Phys. **112,** 2736 (2000).
[54] M. E. Lewittes, C. C. Davis, and R. A. McFarlane, J. Chem. Phys. **69,** 1952 (1978).
[55] R. E. Center, J. Chem. Phys. **58,** 5230 (1973).